On the Optimization of Integrated Terrestrial-Air-Underwater Architecture Using Optical Wireless Communication for Future 6G Network

Priyanka Singh, *Graduate Student Member, IEEE*, Vivek Ashok Bohara, *Senior Member, IEEE*, and Anand Srivastava

***Abstract*—Optical wireless communication (OWC) is one of the promising solution to enhance the capacity of the next generation cellular as well as fiber-wireless (FiWi) broadband access networks. The proposed work aims to complement an OWC system by utilizing unmanned aerial vehicles (UAV) to improve the performance of an integrated terrestrial-air-underwater (TAU) communication framework. Specifically, an integrated FiWi based UAV assisted hybrid free-space optical (FSO) and underwater wireless optical communication (UWOC) system is proposed to meet high data rate requirement between a terrestrial ground station and an autonomous underwater vehicle (AUV). The performance of the proposed scheme is compared against the conventional radio frequency (RF) based TAU communication framework. We also optimize the divergence angle of the optical beam of FSO link using a novel COgnition-based divergence angle tracking (CODAT) algorithm such that the outage probability of FSO links is minimized and the data rate requirement of AUV is also satisfied. The impact of the position of over-sea surface (OSS) relay and UAV altitude on the performance of the proposed system is also analyzed. Through the obtained results it has been shown that the proposed OWC based integrated TAU communication framework outperforms the conventional RF based TAU communication framework.**

***Index Terms*—Free space optics (FSO), underwater wireless optical communications (UWOC), unmanned aerial vehicle (UAV), fiber-wireless (FiWi), outage probability, atmospheric turbulence, pointing error, divergence angle.**

I. Introduction

THE development of sixth-generation (6 G) wireless networks is drawing attention of many researchers. 6G wireless networks are expected to meet high data rate and latency requirements for various bandwidth-intensive applications such as interactive video on demand, streaming 8 K video, and 3D holographic communication. Further, due to rise in human activities in the underwater space, there is a need to provide reliable, robust, and high throughput communication in the underwater oceanic networks especially to submarines, autonomous underwater vehicle (AUV) etc. [1]. Conventionally, the radio frequency (RF) based underwater link is more suitable for short distances and low data rate applications since RF based underwater link has limited bandwidth and suffers from high absorption in the oceanic environment. Acoustic-based underwater link can provide long distance communication in the oceanic environment, however at the expense of increased latency and lower data rate [2], [3]. Consequently, underwater wireless optical communication (UWOC) is a potential solution since it offers high data rates and secure data transmission with low power consumption in an underwater scenario [4].

Fiber-wireless (FiWi) network has emerged as one of the promising solutions for next generation wireless network to meet the stringent requirements of reduced latency and high throughput [5], [6]. In FiWi networks, the benefits of optical fiber based back-end is complemented by the wireless based front-end. Therefore, FiWi is a promising technology that offers not only wide bandwidth but also provides ubiquitous accessibility to the users. In front-end of conventional FiWi, RF based link can be replaced with free space optics (FSO) link to offer robust and high data rate communications. As compared to RF, FSO provides ease of installation, immunity to electromagnetic interference (EMI), a broader unlicensed spectrum, and very high transmission rate. However, atmospheric attenuation, atmospheric turbulence, and pointing errors affect the performance of FSO link. One efficient solution is to use unmanned aerial vehicle (UAV) as an aerial relay with FSO link. UAV assisted FSO link enhances the network's performance in unfavorable atmospheric conditions.

In addition, the optical beam of laser source in FSO link is characterized by divergence angle. The divergence angle of optical beam is an angular measure of the increase in the beam diameter with respect to the distance from the laser source to the receiver aperture. An increase in the divergence angle reduces the outage caused by beam misalignment. However, large divergence angle reduces the received power at the receiver aperture. Therefore, it is essential to optimize the divergence angle to improve the performance of the FSO based communication systems [7], [8].

Manuscript received 22 September 2022; accepted 26 September 2022. Date of publication 29 September 2022; date of current version 13 October 2022. *(Corresponding author: Priyanka Singh.)*

The authors are with Wirocomm Research Group, Department of Electronics & Communication Engineering, Indraprastha Institute of Information Technology Delhi, New Delhi 110020, India (e-mail: priyankas@iiitd.ac.in; vivek.b@iiitd.ac.in; anand@iiitd.ac.in).

Digital Object Identifier 10.1109/JPHOT.2022.3210481

A. Related Work

Some recent works have proposed UAV assisted FSO based communication for the terrestrial-air networks [7], [8], [9], [10], [11]. For instance, in difficult and challenging terrains, UAV assisted relay could be deployed to provide high data rate services. In [7], the authors proposed UAV assisted hybrid FSO and RF based communication system in terrestrial network and optimized the divergence angle of the optical beam to ensure maximum data rate with minimum outage probability. FSO link is used to connect the ground station to UAV, whereas UAV is connected to the ground users via RF links. Consequently, UAV while acting as a relay facilitates the information transfer from the ground station to the mobile users. In [8], the authors optimized the position of the UAV along with the optimal beamwidth under the effect of height and position of building in UAV assisted FSO based communication system. In [9], the authors investigated the performance of UAV assisted backhaul network in which UAV is connected to terrestrial network via FSO link. Moreover, the authors optimized the trajectory of UAV such that flight time of UAV is maximized in order to satisfy a desired data rate. In [10], the authors considered that the ground station transmits the information to UAV through FSO link, and UAV thereafter sends this information to the mobile users using RF links. In addition, the performance of the system is analyzed and the position of UAV under the impact of different atmospheric turbulence is also optimized. In [11], the authors quantified the pointing error under the impact of non-orthogonality of the laser beam and the random fluctuations due to vibrations of the UAV in FSO based communication system. Moreover, the up-link performance in terms of the outage probability and the ergodic rate also analyzed.

Several models have been proposed to provide reliable communication between terrestrial and underwater network. A hybrid FSO and UWOC based communication system has been proposed in [12]. The authors analyzed the performance of the proposed system in terms of outage probability, average bit-error-rate (BER), and average capacity. In [13], the authors analyzed the performance of a multi-user mixed FSO-UWOC system in terms of outage probability. The authors considered that oceanic information collected from the underwater sensors is first transmitted to a static over-sea surface (OSS) relay. Then, this information is relayed to the shore receiver through FSO link. However, the work is limited to FSO and UWOC based terrestrial-underwater cooperative network. Moreover, employing UAV as a terrestrial relay is foreseen as a viable solution to improve the performance of existing terrestrial-underwater communications systems [14]. UAV assisted relay can also assist in oceanography scenarios, where UAV can facilitate connection between the shore transmitter and an AUV. To improve the efficiency of terrestrial-underwater cooperative network, UAV can be employed as an aerial relay to increase the communication range between the shore transmitter and AUV. In [14], the authors analyzed the performance of UAV assisted mixed RF and UWOC based communication systems in terms of outage probability, average BER, and average capacity. In the method proposed, the authors assumed that UAV transmits information to static OSS relay deployed on the sea surface via RF link. Then, OSS relay transmits information to AUV using UWOC link. Table I shows the notable contribution of our work and prior works related to the UAV assisted hybrid system. In [7], [8], [9], [10], and [11], the authors analyzed the performance of UAV assisted FSO based communication system, by taking into account the impact of channel impairments. However, these prior works are limited to terrestrial-air cooperative networks. In [9], a point-to-point FSO link is considered between terrestrial ground station and UAV, the authors focus on maximization of service time under limited energy. In [7], [10], the authors considered that the terrestrial ground station is connected to UAV via FSO link and UAV relays the data to users via a RF link. In [8], it is assumed that UAV works as a relay between terrestrial source node and terrestrial destination node, the authors optimized the position of UAV in the sky. In [11], the authors considered that UAVs transmit the information to multiple mobile users via an RF link and UAVs communicate with the terrestrial ground station via FSO links. Furthermore in [12] and [13], it is assumed that static over-sea surface (OSS) relay transmit the data between terrestrial ground station and an autonomous underwater vehicle (AUV) via FSO-UWOC link. In [14], the authors proposed UAV assisted RF-UWOC based system wherein RF link between UAV and OSS relay and an UWOC link between OSS relay and AUV is considered. Moreover, no communication link between UAV and ground station is considered. Furthermore, unlike [12], [13], and [14] the proposed work optimizes the divergence angle of optical beam for mitigating the effects of misalignment between FSO transmitter and receiver.

In terrestrial-underwater cooperative network, efficient coverage of static ground station largely depends on its locations with respect to the sea surface. On the other hand, deploying UAVs as an aerial relay can effectively alleviate and surpass coverage issues since UAVs are able to flexibly move to the required coverage area. To improve further the efficiency of terrestrial-underwater cooperative network, OSS relay can also be employed as an dynamic relay to increase the coverage range between UAV and AUV. Hence, in this work, we proposed UAV assisted hybrid FSO and UWOC system where UAV and OSS relay can facilitate communication between the ground station and an AUV. Both UAV and OSS serve as relay for further improving the communication range between ground station and AUV. UAV forwards the information from ground station to OSS relay using FSO link. Finally, AUV communicates with dynamic OSS relay using UWOC link.

B. Contribution and Organization

Due to rise in human activities in the underwater, there is a need to provide high throughput communication in the underwater oceanic networks especially to AUV. To meet high data rate requirement for video surveillance, we proposed FiWi based UAV assisted hybrid FSO and UWOC system in terrestrial-underwater cooperative network. Most of the prior works have analyzed the performance of UAV assisted hybrid RF and UWOC link in the air and underwater cooperative networks. However, the performance of UAV assisted hybrid FSO and UWOC in the terrestrial and underwater cooperative networks

TABLE I
COMPARISON OF THE PROPOSED WORK WITH OTHER EXISTING WORKS

Reference	FSO Link	UWOC Link	UAV	Divergence angle analysis	Dynamic movement of UAV	Integrated TAU architecture
[9]	✓	✗	✓	✗	✓	✗
[10]	✓	✗	✓	✗	✓	✗
[7]	✓	✗	✓	✓	✓	✗
[8]	✓	✗	✓	✓	✓	✗
[11]	✓	✗	✓	✗	✓	✗
[12]	✓	✓	✗	✗	✗	✗
[13]	✓	✓	✗	✗	✗	✗
[14]	✗	✓	✓	✗	✓	✗
Proposed work	✓	✓	✓	✓	✓	✓

has not been well investigated yet. Therefore, we have proposed to utilized OWC links such as FSO and UWOC link for providing high data rate between terrestrial station and AUV. However, the joint performance evaluation of UAV assisted FSO and UWOC communication in the terrestrial and underwater cooperative networks has not been investigated yet. Moreover, the prior works have analyzed the performance of the mixed RF and UWOC link in the hybrid network as well derived optimal UAV location in the air-underwater cooperative networks. The future 6G network is expected to offer full integration among terrestrial, air, and underwater communication entities. Therefore, we propose an end-to-end FiWi based UAV assisted hybrid FSO and UWOC system with a decode-and-forward (DF) relaying protocol. In the proposed system, we assume that the optical line terminal (OLT) is located at the central office (CO), which is connected to a passive splitter via feeder fiber. A passive splitter is connected to the number of optical network units (ONUs) via dedicated distribution fiber. Each ONU is equipped with a laser diode (LD) for transmitting information to UAV using FSO link. The UAV serves as an aerial relay and forwards the information to OSS relay using FSO link. Finally, AUV communicates with OSS relay using UWOC link. In addition, we also optimize the divergence angle of the optical beam such that the effect of beam misalignment due to the movement of UAV is mitigated. By optimizing the divergence angle, end-to-end outage probability of FSO link is minimized and data rate requirement of AUV for video surveillance is satisfied. To the best of the author's knowledge, the proposed work is the first of its kind to evaluate the end-to-end performance of an integrated FiWi based UAV assisted hybrid FSO and UWOC system. The performance of the proposed system is investigated by taking into account the impact of the channel impairments such as atmospheric attenuation, pointing errors, atmospheric turbulence, and underwater turbulence. In addition, divergence angle of optical beam in the aerial network is optimized using the proposed COgnition-based divergence angle tracking (CODAT) algorithm. The proposed algorithm is assumed to be aware of thresholds set for end-to-end data rate and outage probability.

The key contributions of the proposed work are summarized as follows:

1) We investigate the end-to-end performance of an integrated FiWi based UAV assisted hybrid FSO and UWOC system in terms of the outage probability. The end-to-end outage performance is analysed in the presence of FSO and UWOC channel impairments.
2) In addition, we derive the analytical expression for the outage probability of the proposed system using FSO and UWOC channel statistics.
3) We propose CODAT algorithm to optimize the divergence angle of the optical beam in such a way that the outage probability of FSO link is minimized and the targeted data rate of AUV is ensured.
4) The impact of mobility of OSS relay and UAV on the performance of the proposed system has been investigated.
5) Moreover, as a performance benchmark, the end-to-end outage performance of the proposed system is compared with a conventional RF based TAU communication system.

The remaining paper is organized as follows: The system model of an integrated FiWi based UAV assisted hybrid FSO and UWOC system is explained in Section II. The channel models considered for the proposed system are presented in Section III. In Section IV, we have discussed the channel statics of FSO and UWOC link. The problem formulation for optimizing the divergence angle and the proposed CODAT algorithm is presented in Section VI. Section VII describes the performance evaluation of an integrated FiWi based UAV assisted hybrid FSO and UWOC system via analytical and simulation results. The concluding remarks of the proposed work are presented in Section VIII.

Notations: Log normal distribution is represented by $\mathcal{X}(\mu, \sigma^2)$, where σ^2 represents the variance and μ is the mean. The Gamma and modified Bessel function of the second kind of order x^{th} are denoted as $\Gamma(\cdot)$ and $K_x(\cdot)$, respectively. erfc$(\cdot)$ and erf$(\cdot)$ denote the complementary error function and error function, respectively.

II. SYSTEM MODEL

Fig. 1 illustrates an integrated FiWi based UAV assisted hybrid FSO and UWOC system in which UAV assisted FSO and UWOC

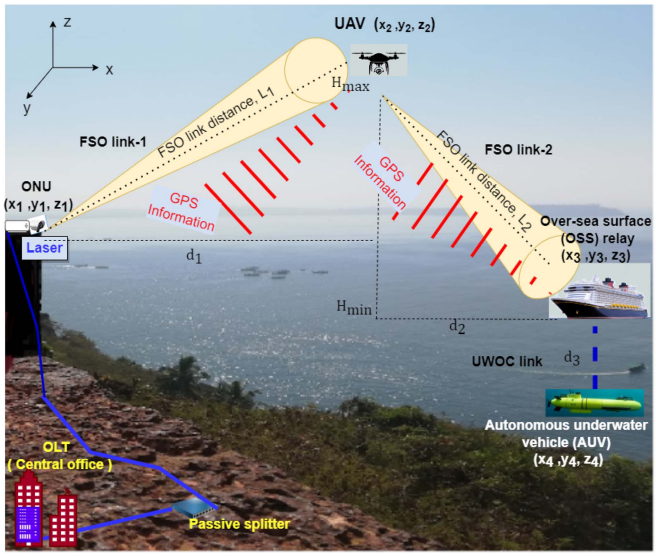

Fig. 1. The proposed integrated FiWi based UAV assisted hybrid FSO and UWOC system.

based front-end network is integrated with 10-Gigabit-passive optical network based back-end network. In back-end network, feeder fiber is used to connect the OLT placed at a CO with passive splitter. Further, the passive splitter is connected to ONUs through a dedicated distribution fiber. We assume that ONU is co-located/connected with a shore transmitter that utilizes a LD for transmitting information to UAV through FSO link. The UAV acts as an aerial relay and forwards the information to the OSS relay using FSO link and the OSS relay further transmits the information to AUV using UWOC link. In this work, we consider three-dimensional cartesian coordinates (x, y, z) for the position of each terminal, such as ONU, UAV, OSS relay, and AUV. We also assume that both UAV and OSS relay utilize the global positioning system (GPS) for sending their location information via beacon messages to ONU and UAV, respectively [15]. After detecting the beacon message from UAV, the distance between UAV and ONU is estimated at ONU. Similarly, the distance between UAV and OSS relay is estimated at UAV. ONU and UAV selects the divergence angle according to the proposed CODAT algorithm for transmitting the optical beam towards UAV and OSS relay, respectively. We also assume that both OSS relay and AUV are mobile. Further, the FSO link between ONU and UAV, and UAV and OSS relay experience atmospheric turbulence, atmospheric attenuation, and pointing errors. In addition, in line with prior literature it is assumed that UWOC link between OSS relay and AUV follows log-normal fading under weak oceanic turbulence [13]. Table II contains all the variables used in the channel modeling and problem formulation.

III. Channel Modeling

This section presents the channel models for FSO and UWOC link as well as the channel impairment factors. FSO link is affected by the channel attenuation due to absorption and scattering of the optical beam, atmospheric turbulence induced by random refractive index fluctuation of the atmosphere, and pointing error caused by beam misalignment between the transmitter and receiver apertures. On the other hand, UWOC link is modeled according to log-normal distribution in the presence of weak oceanic turbulence along with the distance-dependent path loss.

TABLE II
Variables Used in Channel Modeling

Variable	Description
FSO Channel	
α_f, β_f	Scintillation parameters of FSO link f
σ_R^2	Rytov variance
λ	Wavelength of the optical beam
L	UAV based FSO link length
$C_n^2(0)$	Refraction structure parameter in the horizontal link
H_{UAV}	Height of the UAV
k_l	Extinction coefficient related to absorption and scattering
a	Receiver aperture radius
ω_L	Gaussian beam waist of FSO link
ξ	Pointing error coefficient
σ_j	Jitter standard deviation
ω_{Leq}	Equivalent beam waist of FSO link
$\mathcal{BW}_{FSO}$	Bandwidth of FSO link
ϕ	Tilt angle
θ	Divergence angle
δ	Elevation angle
A_{pd}	Effective area of detector
P_t	Transmitted optical power from the laser source
σ_{FSO}^2	Variance of displacement of the optical beam
a	Radius of detector's area
ω_0	Radius of the laser beam at the transmitter
UWOC Channel	
λ_u	Under water optical wavelength
L_u	UWOC link distance between OSS relay and AUV
h_{PL}	Path loss of UWOC link
θ_0	Divergence angle of optical beam in the underwater
$C(\lambda_u)$	Extinction coefficient in UWOC link
h_u	Optical irradiance in UWOC link
A_u	Area of OSS relay aperture
μ_u	Mean of the random variable $\mathcal{X}$
σ_u^2	Variance of the random variable $\mathcal{X}$
$\sigma_{h_a}^2$	Scintillation index of oceanic turbulence
$\mathcal{BW}_{uwoc}$	Bandwidth of UWOC link
$\mathcal{N}_{uwoc}$	PSD of noise in UWOC link
θ_u	Angle between the perpendicular to OSS relay plane and AUV-OSS relay trajectory

A. UAV Based FSO Channel

In the conventional FSO system, FSO transceiver is placed at a fixed location on the top of the building. Unlike the conventional FSO system, UAV based FSO channel is severely affected by the beam misalignment between transmitter and receiver aperture due to the movement and vibrations of UAV [11]. Therefore, UAV based FSO channel is considered as fading channel which is under the impact of atmospheric turbulence (h_{at}), pointing error (h_p), and atmospheric attenuation (h_a). The atmospheric turbulence is assumed to be a random process with Gamma-Gamma distribution, and its probability density function (PDF) is given as [16]:

$$f_{h_{at}}(h_{at}) = \frac{2(\alpha_f\beta_f)^{\frac{\alpha_f+\beta_f}{2}}}{\Gamma(\alpha_f)\Gamma(\beta_f)} h_{at}^{\frac{\alpha_f+\beta_f}{2}-1} K_{\alpha_f-\beta_f}(2\sqrt{\alpha_f\beta_f h_{at}}), \quad (1)$$

where $\Gamma(\cdot)$ and $K_x(\cdot)$ are the Gamma and modified Bessel function of the second kind of order x^{th}, respectively. The scintillation parameters of FSO link f are denoted as α_f and β_f and further expressed as [16]

$$\alpha_f = \frac{1}{\left[\exp\left(\frac{0.49\sigma_R^2}{(1+0.56\sigma_R^{12/5})^{7/6}}\right)-1\right]},$$
$$\beta_f = \frac{1}{\left[\exp\left(\frac{0.51\sigma_R^2}{(1+0.69\sigma_R^{12/5})^{5/6}}\right)-1\right]}, \quad (2)$$

where σ_R^2 is the Rytov variance is denoted as

$$\sigma_R^2 = 1.23 C_n^2 \left(\frac{2\pi}{\lambda}\right)^{7/6} L^{11/6}, \quad (3)$$

where, λ is the wavelength of the optical beam in meters, L is UAV based FSO link length in meters. C_n^2 is the refractive index parameter that characterizes the strength of atmospheric turbulence that lies between 10^{-13} $\mathrm{m}^{-2/3}$ for strong atmospheric turbulence to 10^{-16} $\mathrm{m}^{-2/3}$ for weak atmospheric turbulence [16]. However, for UAV based FSO link, C_n^2 decreases with rise in the height of UAV (up to 3 km) as per Hufnagle-Valley model [10]. C_n^2 is defined as $C_n^2 \approx C_n^2(0)\exp\left(\frac{-H_{UAV}}{100}\right)$, where $C_n^2(0)$ is the refraction structure parameter in the horizontal link and H_{UAV} is the height of UAV. We assumed that ONU is installed at height 100 m of a tower to maintain Line of sight (LoS) transmission between ONU and UAV. Therefore, we consider weak and moderate atmospheric turbulence on FSO link between ONU and UAV. While for FSO link between UAV and OSS relay, we consider strong turbulence. The atmospheric attenuation (h_a) of FSO link over distance L is determined by Beers-Lambert Law as [11], [16]

$$h_a = \exp\left(-k_l L\right), \quad (4)$$

where k_l is the extinction coefficient related to absorption and scattering of the optical beam by particles suspended in the atmosphere (in km^{-1}). The PDF of pointing error is expressed as [16]

$$f_{h_p}(h_p) = \frac{\xi^2}{A_0^{\xi^2}}(h_p)^{\xi^2-1}, \quad (5)$$

where, $A_0 = [\mathrm{erf}(v)]^2$ denotes the fraction of the collected power at radial distance 0 and $v = \frac{\sqrt{\pi}a}{\sqrt{2}\omega_L}$. a is the receiver aperture radius and ω_L is Gaussian beam waist. ξ is the pointing error coefficient, which is defined in terms of jitter standard deviation σ_j and the equivalent beam waist $\omega_{L_{eq}}$ at FSO link distance L as [16]

$$\xi = \frac{\omega_{L_{eq}}}{2\sigma_j}. \quad (6)$$

The PDF of the channel fading due to atmospheric turbulence, atmospheric attenuation, and pointing error is expressed as [16]

$$f_{h_{FSO}}(h) = \frac{\xi^2\alpha_f\beta_f}{A_0 h_a \Gamma(\alpha_f)\Gamma(\beta_f)} G_{1,3}^{3,0}\left(z\middle|\begin{matrix}\xi^2\\ \xi^2-1, \alpha_f-1, \beta_f-1\end{matrix}\right), \quad (7)$$

where $z = \frac{\alpha_f\beta_f h}{A_0 h_a}$, $G_{\cdot,\cdot}^{\cdot,\cdot}(\cdot)$ is the Meijer-G function. The PDF of the instantaneous SNR (γ_{FSO}) of FSO link is expressed as [16]

$$f_{\gamma_{FSO}}(\gamma) = \frac{\xi^2}{2\Gamma(\alpha_f)\Gamma(\beta_f)}\gamma^{-1} G_{1,3}^{3,0}\left(\frac{\alpha_f\beta_f\kappa}{\bar{\gamma}_{FSO}}\gamma\middle|\begin{matrix}\xi^2+1\\ \xi^2, \alpha_f, \beta_f\end{matrix}\right), \quad (8)$$

where $\kappa = \xi^2/(\xi^2+1)$ and $\bar{\gamma}_{FSO}$ is the average electrical SNR. On integrating (8), the corresponding cumulative distribution function (CDF) of the instantaneous SNR of FSO link is expressed as

$$F_{\gamma_{FSO}}(\gamma) = \frac{\xi^2}{\Gamma(\alpha_f)\Gamma(\beta_f)} G_{2,4}^{3,1}\left(\frac{\alpha_f\beta_f\kappa}{\bar{\gamma}_{FSO}}\gamma\middle|\begin{matrix}1, \xi^2+1\\ \xi^2, \alpha_f, \beta_f, 0\end{matrix}\right). \quad (9)$$

B. UWOC Channel

In this paper, UWOC link between OSS relay and AUV is represented as the fading channel under the impact of oceanic turbulence (h_o) and distance dependent path loss (h_{PL}). Path loss (h_{PL}) in oceanic scenario can be estimated as [13]

$$h_{PL} = \frac{A_u\cos\theta_u}{2\pi L_u^2\left(1-\cos\left(\theta_0\right)\right)}\exp\left(-\frac{c\left(\lambda_u\right)L_u}{\cos\theta_u}\right), \quad (10)$$

where λ_u is the wavelength of the optical beam in the underwater in meters, L_u is the length of UWOC link between OSS relay and AUV in meters, and θ_0 is beam divergence angle of laser source. θ_u is the angle between the perpendicular to OSS relay plane and AUV- OSS relay trajectory and A_u is the area of OSS relay aperture.

Oceanic turbulence (h_o) follows log-normal distribution in weak oceanic turbulence as mentioned in [13]

$$f_{h_o}(h_u) = \frac{1}{2h_u\sqrt{2\pi}\sigma_u}\exp\left(-\frac{\left(\ln h_u - 2\mu_u\right)^2}{8\sigma_u^2}\right), \quad (11)$$

where h_u denotes the optical irradiance in the underwater. μ_u and σ_u^2 is the mean and variance of the random variable $\mathcal{X}$, respectively. Random variable $\mathcal{X}$ is expressed as $\mathcal{X} = \frac{1}{2}\ln h_o$. The scintillation index of oceanic turbulence $\sigma_{h_o}^2$ is related to variance of log-normal distribution is expressed as $\sigma_{h_o}^2 = \exp\left(4\sigma_u^2\right) - 1$. The PDF of the instantaneous SNR (γ_{uwoc}) of UWOC link is given as [13]

$$f_{\gamma_{\mathrm{uwoc}}}(\gamma) = \frac{1}{4\gamma\sqrt{2\pi}\sigma_u}\exp\left(-\frac{\left(\ln\left(\frac{\gamma}{\bar{\gamma}_{\mathrm{uwoc}}}\right)-4\mu_u\right)^2}{32\sigma_u^2}\right). \quad (12)$$

On integrating (12), the corresponding CDF of the SNR of UWOC link is expressed as [13]

$$F_{\gamma_{\mathrm{uwoc}}}(\gamma) = \frac{1}{2}\mathrm{erfc}\left(\frac{\ln\left(\frac{\bar{\gamma}_{\mathrm{uwoc}}}{\gamma}\right)+4\mu_u}{4\sqrt{2}\sigma_u}\right). \quad (13)$$

C. End-to-End Data Rate Analysis

In this subsection, the end-to-end performance of the proposed system is analyzed in terms of the achievable data rate. The end-to-end data rate of the proposed system is restricted to the

rate of the weaker link among other links as mentioned in [17]. Thus, the end-to-end data rate of an integrated FiWi based UAV assisted hybrid FSO and UWOC system for DF relaying scheme is given as

$$D_{e2e} = \min\left\{D_{\mathrm{FSO}_1}, D_{\mathrm{FSO}_2}, D_{\mathrm{uwoc}}\right\} \tag{14}$$

where D_{FSO_1} and D_{FSO_2} are the instantaneous achievable data rate of FSO links between ONU and UAV, and UAV and OSS relay, respectively. D_{uwoc} indicates the instantaneous achievable data rate of UWOC link between OSS relay and AUV. In the first FSO link between ONU and UAV, the achievable data rate is calculated as

$$D_{\mathrm{FSO}_1} = \mathcal{BW}_{FSO_1} \log_2(1 + \gamma_{FSO_1}), \tag{15}$$

where $\mathcal{BW}_{FSO_1}$ denotes FSO bandwidth and γ_{FSO_1} is the SNR of FSO link between ONU and UAV. Similarly, we can obtain the data rate for FSO link between UAV and OSS relay as

$$D_{\mathrm{FSO}_2} = \mathcal{BW}_{FSO_2} \log_2(1 + \gamma_{FSO_2}), \tag{16}$$

where $\mathcal{BW}_{FSO_2}$ denotes FSO bandwidth and γ_{FSO_2} is the SNR of FSO link between UAV and OSS relay. In third link between OSS relay and AUV, the achievable data rate is given as

$$D_{\mathrm{uwoc}} = \mathcal{BW}_{\mathrm{uwoc}} \log_2(1 + \gamma_{\mathrm{uwoc}}), \tag{17}$$

where $\mathcal{BW}_{\mathrm{uwoc}}$ denotes bandwidth of UWOC link and γ_{uwoc} is the SNR of UWOC link between OSS relay and AUV.

IV. End to End Outage Probability Analysis

In this section, end-to-end outage probability of the proposed system is derived from the statistical characteristics, i.e., CDF of the end-to-end SNR.

A. Statistical Characteristics of the Channel Links

In this work, we assume that optical beam is transmitted over three independent links in the downlink. Since we use the DF relaying scheme, the analytical expression for SNR of the end-to-end link of the proposed system is given as [18]

$$\gamma_{e2e} = \min\left\{\gamma_{FSO_1},\ \gamma_{FSO_2},\ \gamma_{\mathrm{uwoc}}\right\}, \tag{18}$$

where γ_{FSO_1}, γ_{FSO_2}, and γ_{uwoc} are the SNRs of FSO link between ONU and UAV, UAV and OSS relay, and UWOC link between OSS relay and AUV, respectively.

B. Cumulative Distribution Function

Finally, the CDF of SNR γ_{e2e} of the end-to-end UAV assisted FSO and UWOC based communication system is expressed as [19]

$$F_{\gamma_{e2e}}(\gamma) = 1 - [\left(1 - F_{\gamma_{FSO_1}}(\gamma)\right) \times \left(1 - F_{\gamma_{FSO_2}}(\gamma)\right) \times \left(1 - F_{\gamma_{\mathrm{uwoc}}}(\gamma)\right)], \tag{19}$$

where $F_{\gamma_{FSO_1}}(\gamma)$ denotes the CDF of the SNR of FSO link between ONU and UAV, $F_{\gamma_{FSO_2}}(\gamma)$ denotes the CDF of FSO link between UAV and OSS relay. The analytical expression of CDF of the SNR of the end-to-end UAV-assisted FSO and UWOC system is calculated by substituting (9) and (13) in (19) and is shown in (20). In (20), ξ_1 and ξ_2 denote pointing error coefficient for FSO link between ONU and UAV and UAV and OSS relay, respectively.

$$\begin{aligned} F_{\gamma_{e2e}}(\gamma) = 1 \\ -\Bigg[\left(1-\frac{\xi_1^2}{\Gamma(\alpha_{f_1})\Gamma(\beta_{f_1})}G_{2,4}^{3,1}\left(\frac{\alpha_{f_1}\beta_{f_1}\kappa_1}{\bar{\gamma}_{FSO_1}}\gamma\middle|\begin{matrix}1,\xi_1^2+1\\ \xi_1^2,\alpha_{f_1},\beta_{f_1},0\end{matrix}\right)\right) \\ \times\left(1-\frac{\xi_2^2}{\Gamma(\alpha_{f_2})\Gamma(\beta_{f_2})}G_{2,4}^{3,1}\left(\frac{\alpha_{f_2}\beta_{f_2}\kappa_2}{\bar{\gamma}_{FSO_2}}\gamma\middle|\begin{matrix}1,\xi_2^2+1\\ \xi_2^2,\alpha_{f_2},\beta_{f_2},0\end{matrix}\right)\right) \\ \times\left(1-\frac{1}{2}\mathrm{erfc}\left(\frac{\ln(\frac{\bar{\gamma}_{\mathrm{uwoc}}}{\gamma})+4\mu_u}{4\sqrt{2}\sigma_u}\right)\right)\Bigg], \end{aligned} \tag{20}$$

C. Probability Density Function

The PDF of the SNR of the end-to-end link of the UAV-assisted FSO and UWOC system can be obtained by differentiating (19) and it is expressed as

$$\begin{aligned} f_{\gamma_{e2e}}(\gamma) = &[f_{\gamma_{FSO_1}}(\gamma)\left(1 - F_{\gamma_{FSO_2}}(\gamma)\right)\left(1 - F_{\gamma_{\mathrm{uwoc}}}(\gamma)\right)] \\ &+ [f_{\gamma_{FSO_2}}(\gamma)\left(1 - F_{\gamma_{FSO_1}}(\gamma)\right)\left(1 - F_{\gamma_{\mathrm{uwoc}}}(\gamma)\right)] \\ &+ [f_{\gamma_{\mathrm{uwoc}}}(\gamma)\left(1 - F_{\gamma_{FSO_1}}(\gamma)\right)\left(1 - F_{\gamma_{FSO_2}}(\gamma)\right)], \end{aligned} \tag{21}$$

where $f_{\gamma_{FSO_1}}(\gamma)$ denotes the PDF of the SNR of FSO link between ONU and UAV, $f_{\gamma_{FSO_2}}(\gamma)$ denotes the PDF of FSO link between UAV and OSS relay. The closed form expression of the PDF for the SNR of the end-to-end link of UAV-assisted FSO and UWOC communication system can be obtained by substituting (8), (9), (12), and (13) in (21).

D. Outage Probability

In this subsection, we analyze the outage probability of an integrated FiWi based UAV assisted hybrid FSO and UWOC system. For a particular data rate, when the instantaneous SNR of the end-to-end link of the proposed system falls below the SNR threshold (γ_{th}), the proposed system will suffer an outage. Since no data is received by AUV when received SNR fall below γ_{th}, the outage probability P_{out} can be given as

$$P_{out} = Pr[\gamma_{e2e} < \gamma_{th}]. \tag{22}$$

V. Optimal Divergence Angle Analysis

In this paper, it is assumed that the optical beam of FSO link incident on the detector's plane has Gaussian power intensity profile [11]. Gaussian beam from laser source is directed toward the detector's plane that is perpendicular to its propagation direction [11]. In this work, L denotes FSO link distance between laser source and center of beam footprint on the detector's plane that is perpendicular to its direction of propagation. Fig. 2 depicts geometry of Gaussian beam transmitting from laser source to UAV, where FSO link distance L along the axis of the optical beam is calculated as

$$L = x\cos\left(\theta_{\frac{1}{2}}\right) + AB\cos(\phi) - A'C\cos(\phi), \tag{23}$$

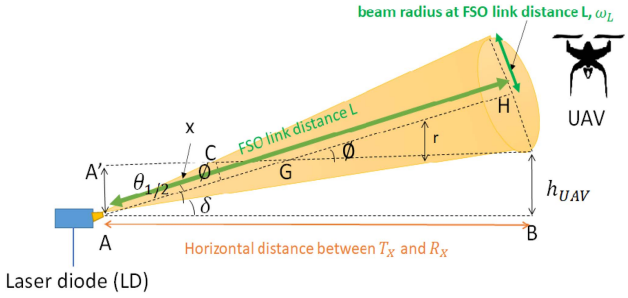

Fig. 2. Geometry for Gaussian beam propagation model.

where $\phi = \delta + \theta_{\frac{1}{2}}$ is tilt angle and $\theta_{\frac{1}{2}}$ denotes half of the divergence angle. x is distance between A and C, the horizontal distance between laser source and detector is denoted by AB, and AA' is the height of UAV from the top of tower at which ONU is installed. r is calculated as $r = L\sin(\phi) - x\sin(\theta_{\frac{1}{2}})$. The elevation angle δ is estimated as

$$\delta = \arctan\left(\frac{AA'}{AB}\right), \tag{24}$$

ω_L is Gaussian beam radius of the optical beam is calculated as [11]

$$\omega_L = \omega_0\sqrt{1 + \left(1 + \frac{2\omega_0^2}{\nu^2(L)}\right)\left(\frac{\lambda L}{\pi\omega_0^2}\right)^2}, \tag{25}$$

where $\omega_0 = \frac{\lambda}{(\pi\theta_{\frac{1}{2}})}$ is the radius of the laser beam at the transmitter. Coherence length in meters is expressed as $\nu(L) = 0.55C_n^2(\frac{2\pi}{\lambda})^2L^{-3/5}$. Hence, the received optical power P_{rec} on the detector's plane from the beam footprint is calculated as [20].

$$P_{\text{rec}} = \frac{2\,P_t A_{pd}}{\pi\,(\omega_L^2)}\exp\left(-\frac{2r^2}{\omega_L^2}\right)10^{\left(\frac{-k_l L}{10}\right)}, \tag{26}$$

where A_{pd} is the effective area of detector as given in [21], P_t is transmitted optical power from the laser source.

A. Problem Formulation

The main objective of the paper is to optimize the divergence angle in such a way that the outage probability of FSO link is minimized and targeted end-to-end data rate is satisfied. The outage probability of FSO link due to beam misalignment between the laser source and detector is estimated as [7]

$$P_{FSO}^{outage} = \exp\left(\frac{-\left(a + \omega_L\right)^2}{2\sigma_{FSO}^2}\right), \tag{27}$$

where σ_{FSO}^2 is the variance of displacement of the optical beam and a is the radius of detector's area. Specifically, the optimization problem is formulated as minimization of the outage probability of FSO link by optimizing the divergence angle of optical beam in (28)

$$(P1): \min_{\theta_1,\theta_2,\delta_1,\delta_2} \quad P_{FSO}^{outage}, \tag{28}$$

$$D_{e2e} \geq D_{req}, \tag{29}$$

$$0^o < \delta_1 \leq 90^o, 0^o < \delta_2 \leq 90^o, \tag{30}$$

$$\theta^{\min} \leq \theta_1 \leq \theta^{\max}, \theta^{\min} \leq \theta_2 \leq \theta^{\max}, \tag{31}$$

$$H^{\min} \leq H_{UAV} \leq H^{\max}, \tag{32}$$

where D_{e2e} is the achieved end-to-end data rate at AUV, D_{req} denotes required end-to-end data rate, which is set to be 100 Mbps that is required for digital video surveillance in oceanic environment monitoring system [22]. δ_1 and δ_2 are elevation angle at ONU and UAV, respectively. θ_1 and θ_2 are the beam divergence angles at ONU and UAV, respectively. H^{min} and H^{max} are the minimum and maximum height of UAV, respectively. θ^{min} and θ^{max} are the minimum and maximum divergence angles of the optical beam at the laser source, respectively.

B. COgnition-Based Divergence Angle Tracking Algorithm (CODAT)

To efficiently solve $(P1)$, we proposed a CODAT algorithm to find the optimal value of divergence angle of the optical beam so that the outage probability of FSO link is minimized and targeted data rate of AUV is guaranteed. The idea of the proposed algorithm is to use the awareness of thresholds of end-to-end data rate and outage probability for optimizing the divergence angle of the optical beam. By optimizing divergence angle of optical beam at laser source, we can further improve the performance of the proposed integrated FiWi based UAV assisted hybrid FSO and UWOC system. With the use of Algorithm 1, both ONU and UAV can estimate the optimal divergence angle for transmitting optical beam towards UAV and OSS relay, respectively. For this work, we assume that divergence angle at ONU and UAV can be changed using either mechanical or non-mechanical beam divergence adjustment techniques that are discussed in [23], [24]. These techniques have wide range of beam divergence angle, accurate divergence control and fast response time. According to Algorithm 1, by using GPS's beacon messages, the location of UAV and OSS relay can be estimated at ONU and UAV, respectively. With this location information, distance between ONU and UAV can be estimated and δ_1 can be calculated using (24). Then, CODAT algorithm dynamically changes the value of θ_1, θ_2 from wide range of beam divergence angle, i.e., from θ^{min} to θ^{max}. FSO link distance between ONU and UAV, L_1 is calculated using (23). For calculating FSO link distance between UAV and OSS relay L_2 and δ_2, we assume AB is equal to the height of UAV from sea surface and AA' is equal to the distance between UAV and OSS relay. Using (25), beam radius at UAV ω_{L_1} and OSS relay ω_{L_2} are calculated. The maximum allowable outage probability for UAV assisted FSO link P_{th} is set to be 10^{-3}. At each iteration, P_{FSO}^{outage} and D_{e2e} are calculated using (27) and (14), respectively. The iteration continues until $P_{FSO}^{outage} \leq P_{th}$ and $D_{e2e} \geq D_{req}$. Finally, the optimal value of θ_1 and θ_2 are updated at ONU and UAV using beam divergence adjustment techniques, respectively.

VI. Results and Discussions

This section shows the end-to-end performance of an integrated FiWi based UAV assisted hybrid FSO and UWOC system and the performance of the proposed CODAT algorithm via

Algorithm 1: COgnition-Based Divergence Angle Tracking Algorithm (CODAT).

Input: d_1, d_2.
1: Calculate δ_1 and δ_2 using (24)
2: Initialize $\theta_1^k = \theta_2^k = [\theta^{min}, \theta^{max}]$
3: **for** k=0, 1, 2...,K **do**
4: Estimate L_1 and L_2 using (23)
5: Calculate ω_{L_1} and ω_{L_2} using (25)
6: Compute P_{FSO}^{outage} from (27)
7: **if** $P_{FSO}^{outage} \leq P_{th}$ **then** calculate D_{e2e}
8: **else** $\theta^k = \theta^{k+1}$, Go to step 4
9: **end if**
10: **if** $D_{e2e} \geq D_{req}$ **then** $\theta^{optimal} = \theta^k$
11: **else** $\theta^k = \theta^{k+1}$, Go to step 4
12: **end if**
13: **end for**
14: **return** $\theta_1^{optimal}, \theta_2^{optimal}$

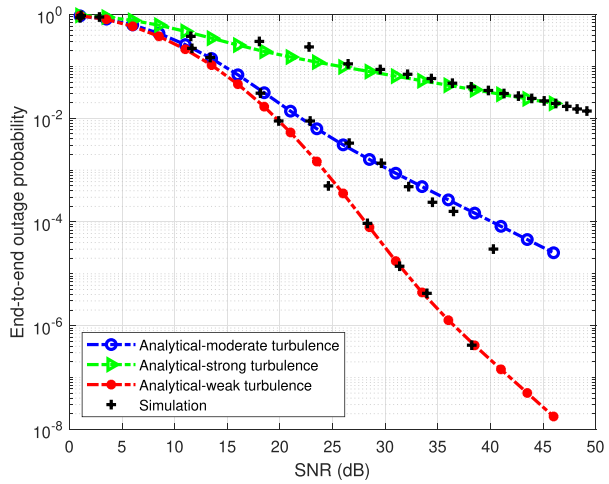

Fig. 3. End-to-end outage probability of an integrated FiWi based UAV assisted hybrid FSO and UWOC framework over weak, moderate and strong turbulence with pointing errors.

Monte Carlo simulations. We set the SNR threshold $\gamma_{th} =$ 2 dB for the analysis of end-to-end outage performance [14]. In order to see the impact of atmospheric turbulence on FSO link, we calculate the values of Gamma-Gamma fading parameters α_f and β_f using (2). The parameter related to pointing error ξ is calculated using (6). The effect of pointing error is more pronounced with smaller value of ξ. The parameters used for simulations are presented in Table III.

TABLE III
SIMULATION PARAMETERS [13], [16], [23], [25], [26]

Parameters	Values
FSO Channel	
Optical wavelength, λ	1550 nm
Position of ONU (x_1, y_1, z_1)	(0, 0, 100) m
Final position of UAV (x_2, y_2, z_2)	(500, 0, 150) m
Initial position of OSS relay (x_3, y_3, z_3)	(1000, 0, 4) m
FSO transmit optical power, P_t	40 W
Refractive index structure, $C_n^2(0)$ (moderate turbulence)	5×10^{-14} $m^{-2/3}$
Refractive index structure, $C_n^2(0)$ (strong turbulence)	1×10^{-13} $m^{-2/3}$
Refractive index structure, $C_n^2(0)$ (weak turbulence)	8×10^{-15} $m^{-2/3}$
Minimum divergence angle (θ^{min})	0.05 mrad
Maximum divergence angle (θ^{max})	1.5 mrad
Receiver aperture radius, a	5 cm
PD responsivity	0.5 A/W
Jitters standard deviation, σ_j	30 cm
PD area, A_{pd}	7 mm^2
Refractive index, RI	1.5
Receiver half-angle field-of-view	5.15^o
Gain of optical filter, $U(\phi)$	1
Extinction coefficient, k_l	0.43
Noise variance, $\sigma_{n_{01}}^2$	10^{-14}
Bandwidth of FSO link, $\mathcal{BW}_{FSO}$	625 MHz
UWOC Channel	
Under water optical wavelength, λ_u	532 nm
Under water link distance, d_3	1-10 m
Initial position of AUV (x_4, y_4, z_4)	(1000, 0, d_3) m
Divergence angle in the underwater, θ_0	10^o
θ_u	5^o
$C(\lambda_u)$ for clear ocean water	0.151
Transmit optical power	0.1 W
Area of OSS relay aperture, A_u	1.7×10^{-4} per m^2
Optical to electric power conversion coefficient	1 A/W
Bandwidth of UWOC link, $\mathcal{BW}_{uwoc}$	150 MHz
PSD of noise, $\mathcal{N}_{uwoc}$	1.6×10^{-14} W/Hz
RF Channel	
Transmit power	0.1 W
Bandwidth	625 MHz
Pathloss coefficients (A, B)	(-1.5, 3.5)
Ricican factor coefficient, K(0)	5 dB
PSD of noise	2.57×10^{-12} W/Hz
Ricican factor coefficient, K(π/2)	15 dB
RF based underwater Channel	
Operating frequency	420 MHz
Underwater link distance, d_3	1-10 m
Conductivity, σ	0.075 m^{-1}
Permeability, μ	1.2566×10^{-6} Hm^{-1}
Permittivity, ϵ	6.8588×10^{-10} Fm^{-1}
Transmit power	0.1 W
Bandwidth	100 MHz
PSD of noise	4.0×10^{-13} W/Hz

A. Outage Probability

Fig. 3 shows the end-to-end outage probability with respect to the SNR of the end-to-end link under the impact of atmospheric loss, pointing error, and atmospheric turbulence for both FSO links between ONU and UAV, and UAV and OSS relay. Analytical derivation obtained in 20 is validated through simulations. The end-to-end outage performance of the proposed

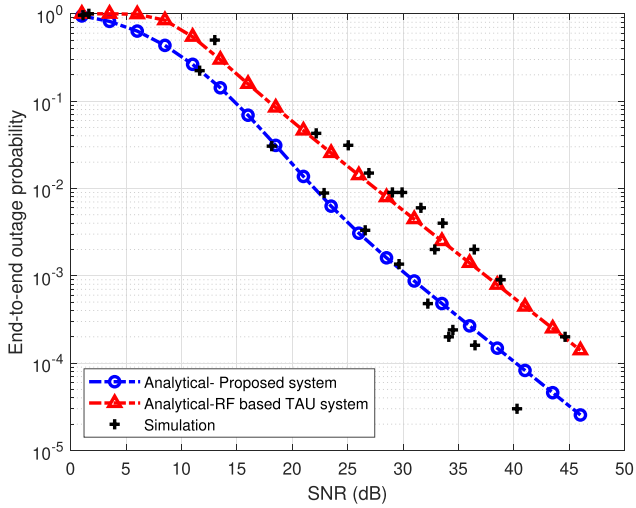

Fig. 4. Comparison of end-to-end outage probability of an integrated FiWi based UAV assisted hybrid FSO and UWOC system with conventional RF based TAU communication framework.

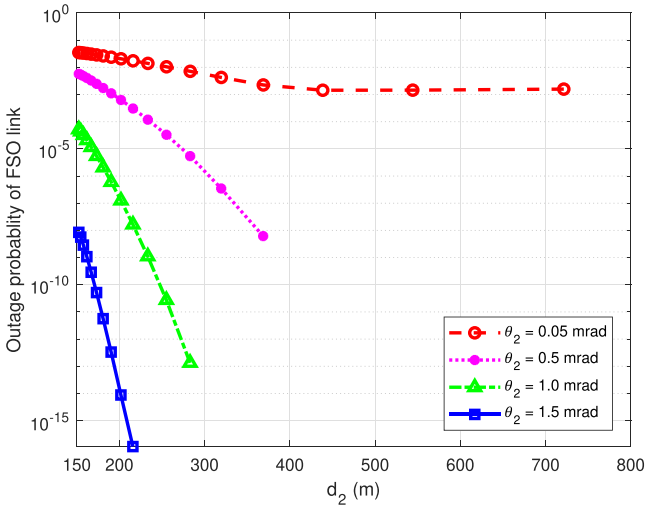

Fig. 5. End-to-end outage probability of FSO link versus FSO link distance between UAV and OSS relay, d_2 for different divergence angles.

system in weak and moderate turbulence is much better than strong turbulence. Strong turbulence degrades the outage performance of the proposed system. For instance, the outage probability of 10^{-1} is achieved at 15 dB SNR and 13.5 dB SNR in moderate turbulence with pointing error (ξ_1=1.01, ξ_2=0.7) and weak turbulence with pointing error (ξ_1=1.45, ξ_2=1.03), respectively. While in the case of strong turbulence with pointing error (ξ_1=0.6, ξ_2=0.47), the outage probability of 10^{-1} is achieved at 25 dB SNR. Moreover, in the case of moderate turbulence, the outage probability of 10^{-3} can be achieved at 30 dB SNR. For comparison, we consider conventional RF based TAU communication framework in which channel between ONU and UAV, and UAV and OSS relay are RF link, respectively. Further, OSS relay is connected to AUV using RF based underwater link. We consider that RF channel between ONU and UAV, and UAV and OSS relay experience rician fading due to presence of strong LoS path. The RF based channel is modeled according to [26]. We also assume that under water link between OSS relay and AUV is RF based underwater link as given in [25]. The considered simulation parameters related to conventional RF based TAU communication framework are listed in Table III. Fig. 4 shows the end-to-end outage performance of both integrated FiWi based UAV assisted hybrid FSO and UWOC system and conventional RF based TAU communication framework. It can be observed that the proposed system outperforms the conventional RF based TAU communication framework, specifically in moderate turbulence with pointing error. The outage probability of 10^{-3} is achieved at 30 dB and 37 dB SNR for the proposed system and conventional RF based TAU communication framework, respectively.

B. Performance Evaluation of CODAT Algorithm

For investigating the performance of CODAT under moderate turbulence conditions with pointing error (ξ_1=1.01, ξ_2 = 1.01), we consider the standard deviation of beam displacement $\sigma_{FSO} = 0.015$. We also assume that distance between UAV and

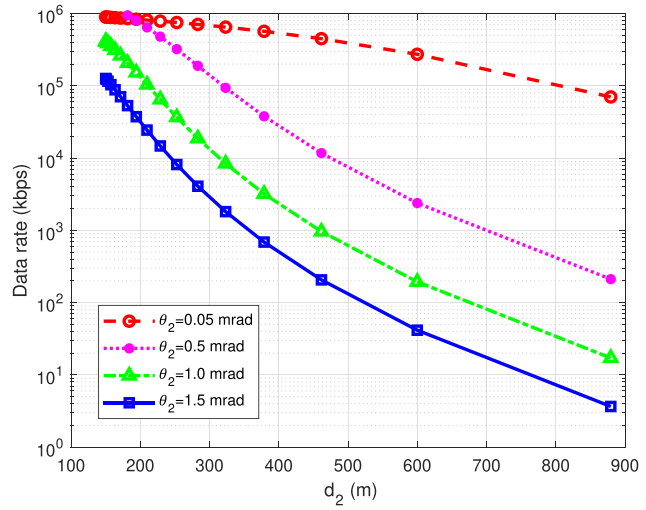

Fig. 6. Data rate between OLT and OSS relay versus FSO distance between UAV and OSS relay, d_2.

OSS relay is dynamically changing due to movement of OSS relay. Fig. 5 depicts that variation of P_{FSO}^{outage} with respect to change in d_2, when $d_1 = 455$ m, $\theta_1 = .05$ mrad. From Fig. 5, it can be observed that P_{FSO}^{outage} decreases with increase in beam divergence angle θ_2. However, for a smaller distance between UAV and OSS relay, outage probability of less than 10^{-3} is achieved. By reducing θ_2, large distance between UAV and OSS relay can be achieved. For instance, at $\theta_2 = 0.05$ mrad and $d_2 = 720$ m, an outage probability of 10^{-3} is achieved. Whereas for $\theta_2 = 1.5$ mrad, $P_{FSO}^{outage} \leq 10^{-3}$ is achieved for very short distance $d_2 = 220$ m. Therefore, there is trade-off between transmission distance and FSO outage.

Fig. 6 shows the end-to-end data rate for different θ_2, when $d_1 = 455$ m and $\theta_1 = .05$ mrad. It is obvious that the targeted data rate of 100 Mbps can be achieved at OSS relay when $\theta_2 = 0.05$ mrad is selected because a smaller divergence angle results in lower pointing error. While higher value of θ_2 results in higher pointing error. Hence, the targeted data rate of 100 Mbps

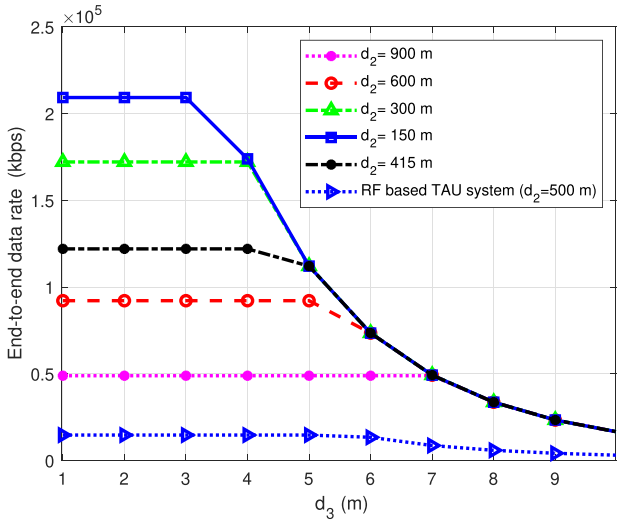

Fig. 7. End-to-end data rate of an integrated FiWi based UAV assisted hybrid FSO and UWOC system versus underwater link distance between OSS relay and AUV, d_3 with $\theta_2 = 0.05$ mrad.

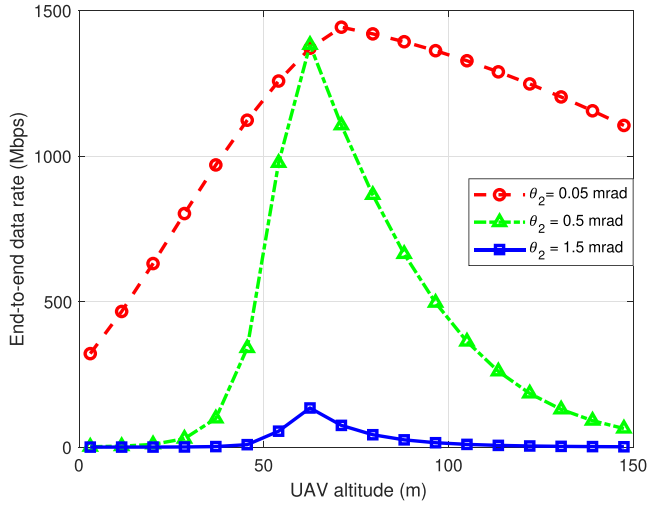

Fig. 8. Data rate of FSO link between OLT and OSS relay versus UAV altitude.

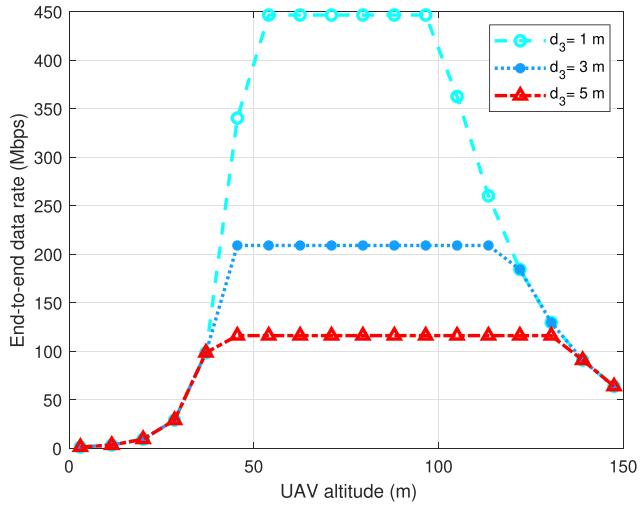

Fig. 9. End-to-end data rate of an integrated FiWi based UAV assisted hybrid FSO and UWOC system versus UAV altitude with $\theta_2 = 0.05$ mrad.

is not achieved at a large divergence angle. Moreover, for smaller values of θ_2, the distance between OSS relay and UAV can be extended. At $\theta_2 = 0.05$ mrad, the data rate requirement of 100 Mbps at OSS relay is achieved with $d_2 = 800$ m.

It can be observed from Fig. 7, as the underwater distance between OSS relay and AUV d_3 increases from 1 m to 10 m, the end-to-end data rate decreases with respect to d_3. When $d_3 = 5$ m and $\theta_2 = 0.05$ mrad, more than 200 Mbps end-to-end data rate is achieved at $d_2 = 415$ m. It is also observed that for short distance between UAV and OSS relay, higher end-to-end data rate can be achieved. While with large d_2, i.e., more than 600 m, desired end-to-end data rate at AUV is not achieved. Moreover, as a benchmark for comparison, the end-to-end rate performance of the proposed system is compared with conventional RF based TAU communication framework. It can be observed that conventional RF based TAU communication framework is not performing well, specifically in terms of end-to-end data rate. The required end-to-end data rate can not be achieved using conventional RF based TAU communication framework. Therefore, an integrated FiWi based UAV assisted hybrid FSO and UWOC system outperforms conventional RF based TAU communication framework, specifically for small beam divergence angles. At fixed $d_3 = 5$ m, an integrated FiWi based UAV assisted hybrid FSO and UWOC system outperforms conventional RF based TAU communication framework, specifically for data rate upto 100 Mbps. At least up to $d_2 = 415$ m, more than 100 Mbps data rate can be achieved at AUV with $\theta_d = 0.05$ mrad. In the case of $\theta_2 = 0.1$ mrad, the end-to-end data rate of 100 Mbps is achieved for short distance $d_2 = 205$ m. As compared to the proposed system, conventional RF based TAU communication framework is not performing well as it achieves less than 40 Mbps end-to-end data rate when $d_2 = 500$ m and $d_3 = 6$ m. Therefore, there is trade-off between the end-to-end data rate and the distance between UAV and OSS relay d_2 for both the framework.

To investigate the impact of UAV altitude on the data rate at OSS relay, we plot data rate versus the UAV altitude in Fig. 8, when $d_1 = 455$ m, $d_2 = 550$ m. The data rate at OSS relay at $\theta_2 = 0.05$ mrad reaches maximal value at UAV altitude = 70 m. Since at this UAV altitude, strong LoS is maintained between ONU and UAV and distance between UAV and OSS relay is not much large. On the other hand, at high UAV altitudes, the data rate performance at OSS relay degrades as distance between ONU and UAV, and UAV and OSS relay increases. However for higher values of θ_2, the data rate degrades with respect to rise in height of UAV. Fig. 9 depicts the end-to-end data rate performance of the proposed system as function of UAV altitude with $\theta_1 = \theta_2 = 0.05$ mrad. For $d_3 = 1$ m, $d_{e2e} = 450$ Mbps can be achieved when UAV operates at height of 56 m to 95 m. While in the case of $d_3 = 5$ m, an end-to-end data rate greater than 100 Mbps is achieved, when UAV altitude increases from 45 m to 130 m. Fig. 10 shows the end-to-end data rate versus d_2 for both UAV-assisted FSO and UWOC

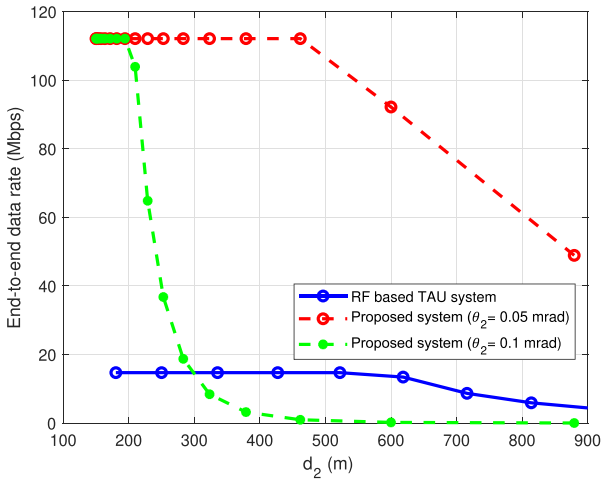

Fig. 10. Comparison of end-to-end data rate of an integrated FiWi based UAV-assisted FSO and UWOC system against conventional RF based TAU communication framework.

system and conventional RF based communication framework, when $d_3 = 5$ m. It is observed that as compared to RF based system, the proposed system can achieve more than 100 Mbps up to $d_2 = 415$ m, when $\theta_2 = 0.05$ mrad. With higher value of $\theta_2 = 0.1$ mrad, the end-to-end data rate of 100 Mbps is achieved at short distance of $d_2 = 200$ m. Conventional RF based TAU communication system always achieves less than 20 Mbps data rate. The proposed UAV-assisted FSO and UWOC system has a better performance than conventional RF based TAU communication framework in terms of the end-to-end data rate since the impairment due to pointing errors caused due to beam misalignment between transmit and receive apertures has been compensated. Specifically, for alleviating the effect of beam misalignment, we have optimized the divergence angle of optical beam using CODAT algorithm. The CODAT algorithm finds the optimal value of divergence angle of the optical beam such that the outage probability of FSO link is minimized and data rate requirement of AUV for video surveillance is satisfied.

VII. Conclusion

In this paper, we proposed an OWC based integrated TAU communication framework for future 6G network. Specifically, we analyzed the end-to-end performance of an integrated FiWi based UAV assisted hybrid FSO and UWOC system in terms of the outage probability under the impact of FSO and UWOC channel impairments. FSO link is assumed to experience gamma-gamma distribution fading with pointing error, whereas UWOC link followed log-normal distribution fading with distance dependent path loss. In addition, the analytical expression of the outage probability of the proposed system is derived and validated through simulations. The end-to-end performance of the proposed system is compared with conventional RF based TAU communication framework in terms of the outage probability. In addition, we formulated the optimization problem to optimize the divergence angle of the optical beam such that the outage performance of FSO link between ONU and OSS relay is minimized and targeted data rate of AUV is ensured. We solved the proposed optimization problem using a novel CODAT algorithm. It was demonstrated that the beam misalignment in FSO link due to movement of UAV can be mitigated by using small beam divergence angle. However, the end-to-end data rate is achieved within limited transmission distances between UAV and OSS relay since there is always a trade off between transmission distance and achievable data rate. Our simulation results revealed the optimal transmission range between UAV and OSS relay, and OSS relay and AUV for the improved end-to-end performance. In future, the proposed work can be extended to include the evaluation with respect to multi-AUVs scenarios.

References

[1] Z. Zhang et al., "6G wireless networks: Vision, requirements, architecture, and key technologies," *IEEE Veh. Technol. Mag.*, vol. 14, no. 3, pp. 28–41, Sep. 2019.
[2] H. Kaushal and G. Kaddoum, "Underwater optical wireless communication," *IEEE Access*, vol. 4, pp. 1518–1547, 2016.
[3] Z. Zeng, S. Fu, H. Zhang, Y. Dong, and J. Cheng, "A survey of underwater optical wireless communications," *IEEE Commun. Surv. Tut.*, vol. 19, no. 1, pp. 204–238, Jan.–Mar. 2017.
[4] S. Dang, O. Amin, B. Shihada, and M.-S. Alouini, "What should 6G be," *Nature Electron.*, vol. 3, no. 1, pp. 20–29, 2020.
[5] H. Guo, Y. Wang, J. Liu, and N. Kato, "Super-broadband optical access networks (OANs) in 6G: Vision, architecture, and key technologies," *IEEE Wireless Commun.*, early access, May 9, 2022, doi: 10.1109/MWC.007.2100550.
[6] M. Maier, "Toward 6G: A new era of convergence," in *Proc. Opt. Fiber Commun. Conf.*, 2021, pp. F4H–1.
[7] T. Zhang, X. Sun, and C. Wang, "On optimizing the divergence angle of an FSO based fronthaul link in drone assisted mobile networks," *IEEE Internet Things J.*, vol. 9, no. 9, pp. 6914–6921, May 2022.
[8] M. T. Dabiri and S. M. S. Sadough, "Optimal placement of UAV-assisted free-space optical communication systems with DF relaying," *IEEE Commun. Lett.*, vol. 24, no. 1, pp. 155–158, Jan. 2020.
[9] J.-H. Lee, K.-H. Park, Y.-C. Ko, and M.-S. Alouini, "A UAV-mounted free space optical communication: Trajectory optimization for flight time," *IEEE Trans. Wireless Commun.*, vol. 19, no. 3, pp. 1610–1621, Mar. 2020.
[10] H. Ajam, M. Najafi, V. Jamali, and R. Schober, "Ergodic sum rate analysis of UAV-based relay networks with mixed RF-FSO channels," *IEEE Open J. Commun. Soc.*, vol. 1, pp. 164–178, 2020.
[11] M. Najafi, H. Ajam, V. Jamali, P. D. Diamantoulakis, G. K. Karagiannidis, and R. Schober, "Statistical modeling of the FSO fronthaul channel for UAV-based communications," *IEEE Trans. Commun.*, vol. 68, no. 6, pp. 3720–3736, Jun. 2020.
[12] L. Yang, Q. Zhu, S. Li, I. S. Ansari, and S. Yu, "On the performance of mixed FSO-UWOC dual-hop transmission systems," *IEEE Wireless Commun. Lett.*, vol. 10, no. 9, pp. 2041–2045, Sep. 2021.
[13] C. Christopoulou, H. G. Sandalidis, and I. S. Ansari, "Outage probability of a multisensor mixed UOWC–FSO setup," *IEEE Sens. Lett.*, vol. 3, no. 8, pp. 1–4, Aug. 2019.
[14] S. Li, L. Yang, D. B. da Costa, and S. Yu, "Performance analysis of UAV-based mixed RF-UWOC transmission systems," *IEEE Trans. Commun.*, vol. 69, no. 8, pp. 5559–5572, Aug. 2021.
[15] H.-J. Moon, H.-B. Jeon, and C.-B. Chae, "RF lens antenna array-based one-shot coarse pointing for hybrid RF/FSO communications," *IEEE Wireless Commun. Lett.*, vol. 11, no. 2, pp. 240–244, Feb. 2022.
[16] S. Sharma, A. Madhukumar, and R. Swaminathan, "Effect of pointing errors on the performance of hybrid FSO/RF networks," *IEEE Access*, vol. 7, pp. 131418–131434, 2019.
[17] A. El Gamal and Y.-H. Kim, *Network Information Theory*. Cambridge, U.K.: Cambridge Univ. Press, 2011.

[18] N. I. Miridakis, M. Matthaiou, and G. K. Karagiannidis, "Multiuser relaying over mixed RF/FSO links," *IEEE Trans. Commun.*, vol. 62, no. 5, pp. 1634–1645, May 2014.
[19] A. Papoulis and S. U. Pillai, *Probability, Random Variables, and Stochastic Processes, New*. Tata York, NY, USA: McGraw-Hill Education, 2002.
[20] Q. Fan, N. Ansari, J. Feng, R. Rojas-Cessa, M. Zhou, and T. Zhang, "Reducing the number of FSO base stations with dual transceivers for next-generation ground-to-train communications," *IEEE Trans. Veh. Technol.*, vol. 67, no. 11, pp. 11143–11153, Nov. 2018.
[21] Y. Kaymak, R. Rojas-Cessa, J. Feng, N. Ansari, and M. Zhou, "On divergence-angle efficiency of a laser beam in free-space optical communications for high-speed trains," *IEEE Trans. Veh. Technol.*, vol. 66, no. 9, pp. 7677–7687, Sep. 2017.
[22] M. Kong et al., "Real-time optical-wireless video surveillance system for high visual-fidelity underwater monitoring," *IEEE Photon. J.*, vol. 14, no. 2, Apr. 2022, Art. no. 7315609.
[23] K. H. Heng, W.-D. Zhong, T. H. Cheng, N. Liu, and Y. He, "Beam divergence changing mechanism for short-range inter-unmanned aerial vehicle optical communications," *Appl. Opt.*, vol. 48, no. 8, pp. 1565–1572, 2009.
[24] V. V. Mai and H. Kim, "Non-mechanical beam steering and adaptive beam control using variable focus lenses for free-space optical communications," *J. Lightw. Technol.*, vol. 39, no. 24, pp. 7600–7608, 2021.
[25] D. Park, K. Kwak, W. K. Chung, and J. Kim, "Development of underwater short-range sensor using electromagnetic wave attenuation," *IEEE J. Ocean. Eng.*, vol. 41, no. 2, pp. 318–325, Apr. 2016.
[26] M. M. Azari, F. Rosas, K.-C. Chen, and S. Pollin, "Ultra reliable UAV communication using altitude and cooperation diversity," *IEEE Trans. Commun.*, vol. 66, no. 1, pp. 330–344, Jan. 2018.